CONFERENCE PRE-PRINT

DENSITY LIMIT DISRUPTION INDUCED BY CORE LOCALIZED ALFVENIC ION TEMPERATURE GRADIENT INSTABILITIES IN A TOROIDAL PLASMA

W. Chen^{1*}, L. W. Hu¹, P. W. Shi¹, T. Long¹, J. Q. Xu¹, R. R. Ma¹, Y. G. Li¹, L. M. Yu¹, X. Yu¹, M. Jiang¹, T. F. Sun¹, J.M. Gao¹, Y. B. Dong¹ and Z. B. Shi¹

¹Southwestern Institute of Physics, P.O. Box 432 Chengdu 610041, China

Corresponding Author: chenw@swip.ac.cn

Abstract:

The density limit is a mysterious barrier to magnetic confinement nuclear fusion, hitherto, and is still an unresolved issue. In this letter, we will present the experimental results of the density limit and core-localized kinetic MHD instabilities on HL-2A. Firstly, the high density discharges with $ne/ne_G > 1$ have been achieved by the conventional gas-puff fuelling method in Ohmic heating plasmas, and the corresponding duration time is close to $t \sim 500~{\rm ms} \sim 30\tau_E$, where τ_E is the global energy confinement time. Secondly, it is found for the first time that there are multiple MHD instabilities in the core plasmas while $ne/ne_G \sim 1$. The analysis suggests that the core localized MHD activities belong to Alfvénic ion temperature gradient (AITG) modes or kinetic ballooning modes (KBMs), and firstly it is found on experiment that they trigger the minor or major disruption of bulk plasmas while the density is peaked. These new findings are of great importance to figure out and understand the origin of the density limit.

Introduction.—High plasma density (ne) is essential for accessing high fusion gain since the fusion power density (P) scales as $P \propto ne^2$. However, there is a limit (known as Greenwald limit) for tokamak high density discharges[1, 2]. The Greenwald limit is an empirical limit for the achievable line-averaged plasma density on experiments, namely $ne_G = I_p/\pi a^2$, where ne_G is the line-averaged plasma density in units of $10^{20}m^{-3}$, I_p the plasma current in MA and a the minor radius in m. Generally, when the Greenwald density is reached, the bulk plasma frequently disrupts as well as the discharge halts. Therefore, the density limit represents an operational limit for tokamaks. Before the density limit disruption, tearing mode instability often occurs. It is generally believed that this is caused by an increased current gradient resulting from current quenching after edge cooling[3, 4]. However, this does not explain the reason for the restriction on the rise of core density, nor does it account for density limit disruptions that occur in the absence of tearing modes. The Alfvén ion temperature gradient (AITG) mode was discovered in the SOC stage of ohmically heated plasmas in the HL-2A tokamak[5]. These instabilities may be related to the degradation of plasma confinement. Experimentally, the AITG can also be referred to as the Kinetic Ballooning Mode (KBM). Simulation results from various codes indicate that the excitation of KBM/AITG has a beta (pressure ratio) threshold and becomes more unstable under conditions of weak magnetic shear [6, 7, 8].

Core-localized KBM/AITG instabilities occur prior to density limit disruption.—A high-density operation mode with plasma density exceeding the Greenwald density limit has been achieved on the HL-2A tokamak through gas puffing fueling. Figure 1 shows the time series plots of plasma parameters for discharge #38522. During the period from 800

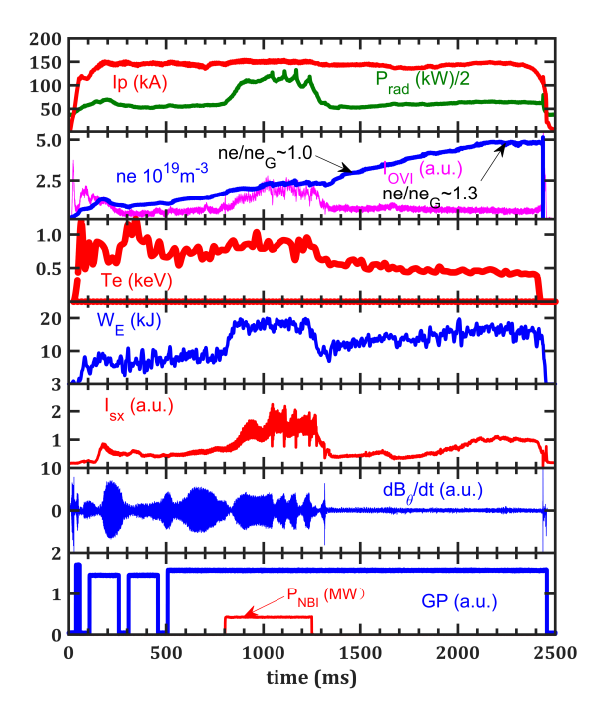


FIG. 1: Time-series plots of plasma parameters for discharge #38522. The plasma current Ip, total radiation power of plasma P_{rad} , line-averaged electron density ne, oxygen impurity level I_{OVI} , carbon impurity level I_{CIII} , core electron temperature Te (red line), plasma stored energy W_E , soft X-ray (SXR) signal I_{SX} , Time-differential poloidal magnetic perturbation dB_{θ}/dt , gas-puffing signal GP and NBI power P_{NBI} are labeled in the figure. The black arrows in the figure indicate the moments when the ratio of plasma density to the Greenwald density limit, ne/neG, reaches 1 and its maximum value.

ms to 1250 ms, discharge #38522 has about 0.5 MW of NBI power. The plasma current $Ip \sim 150$ kA for shot #38522. And the corresponding Greenwald density limit ne_G is about $3.0 \times 10^{19} \mathrm{m}^{-3}$, by assuming minor radius of plasma a = 0.4 m. The maximum lineaveraged electron density reaches about $ne = 5.0 \times 10^{19} \mathrm{m}^{-3}$. The maximum Greenwald density limit fraction ne/ne_G is about 1.3, as labeled in figure 1. The plasma exceeded the Greenwald density limit for durations exceeding 500 ms, equivalent to approximately 30 times the energy confinement time τ_E . It can be seen that the Greenwald density limit is not a strict constraint on plasma density. The possible reasons for shot #38522 achieving such high Greenwald density limit fraction could be the relatively low impurity levels in the plasma and comparatively weaker plasma instabilities. As shown in the time-series plots of impurity levels (I_{OVI}) and radiation power (P_{rad}) in figure 1, the overall radiation and impurity levels of the plasma do not exhibit a significant increase prior to the density limit disruption. Strong MHD modes are found in the magnetic perturbation signal before 1300 ms in discharge #38522, but not before the density disruption at about 2500 ms.

The density profiles of shot #38522 are shown in figure 2(a). As the line-averaged density increases, the plasma density profile exhibits a peaking trend. Especially in the core region of plasma, the density gradient increases obviously. The core electron density prior to density limit disrution is about $8.2 \times 10^{19} \text{m}^{-3}$. Figure 2(b) is the spectrum of microwave interferometer signal for shot #38522. The electron density exceeded Greenwald density after 1900 ms for shot #38522. Multiple instabilities emerge in the spectrum after 2100 ms, with frequency from near zero frequency up to 150 kHz. Two-channel microwave

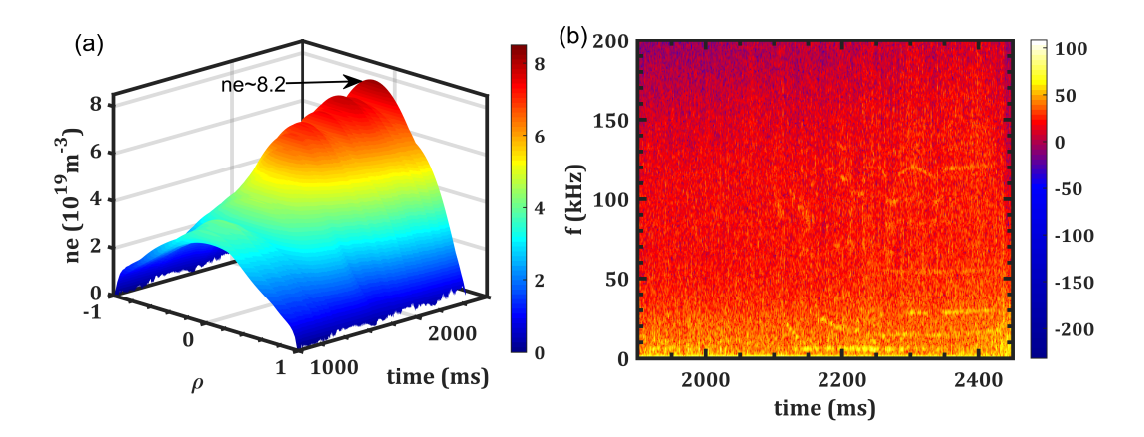


FIG. 2: (a) Time evolution diagram of the density profile for shot #38522, where the density profile is derived from the Abel inversion results of laser interference signals. (b) The microwave interference signal spectrum prior to the density limit disruption in shot #38522, showing instabilities within the frequency range of 0-130 kHz.

interferometer has been installed on the HL-2A tokamak, positioned at z = 0 cm and z = 15 cm respectively, for horizontal injection into the plasma, where z represents the longitudinal coordinate of the plasma. Signals in figure 2(b) come from z = 0 cm channel of microwave interferometer. But in z = 15 cm channel of microwave interferometer's spectrum, these instabilities can also be observed. This suggests that these instabilities are also distributed in the region where r > 15 cm. Since instabilities similar to those observed in figure 2(b) cannot be detected in the spectra obtained from other diagnostic tools such as magnetic probes, it is speculated that these instabilities may be located in the plasma core region, rendering them undetectable by magnetic probes. The TAE[9] frequency at q=2 surface is about 96 kHz during the shown time period in figure 2(b). The instabilities in the spectrum can be roughly categorized into two types based on frequency: one type consists of modes near 100 kHz, and the other type comprises modes below 30 kHz. The former have a similar frequency to TAE. The latter, with frequencies approximately ranging from 0 to 1/3 f_{TAE} , is more likely to be a type of instability known as KBM or alternatively referred to as AITG or beta-induced Alfvén eigenmode (BAE)[10, 11]. There is a particle energy threshold for driving TAE, while there is a lack of energetic particle sources in ohmic heating plasma[12]. Therefore, the instabilities whose frequency is close to TAE frequency may not be TAE instabilities.

Figures 3(a1-a2) are raw signals of SXR for shot #38522. Figure 3(a1) is the time period without instabilities in microwave interferometer spectrum and Figure 3(a2) is the time period with instabilities in microwave interferometer spectrum. The presence of sawtooths in the spectrum indicates that there is a q=1 surface at this time. And the SXR level I_{SX} increases with time, which comes from increase of plasma density. The SXR level in figure 3(a2) decreases slowly with time, and the density increases with time as shown in figure 2(a). Since the amplitude of SXR $I_{SX} \propto ne^2 \sqrt{Te}$, and the SXR signal mainly comes from bremsstrahlung in plasma[13]. So the decrease in SXR level comes from decrease of electron temperature. The figure 3(a3) shows that the fast-growing m/n=-2/-1 tearing mode lead to density limit disruption. These instabilities only exist when there is not any sawtooth or q=1 surface. Therefore, the safety factor profile or magnetic configuration of the plasma may have a significant influence on the core-localized MHD instabilities preceding the density limit.

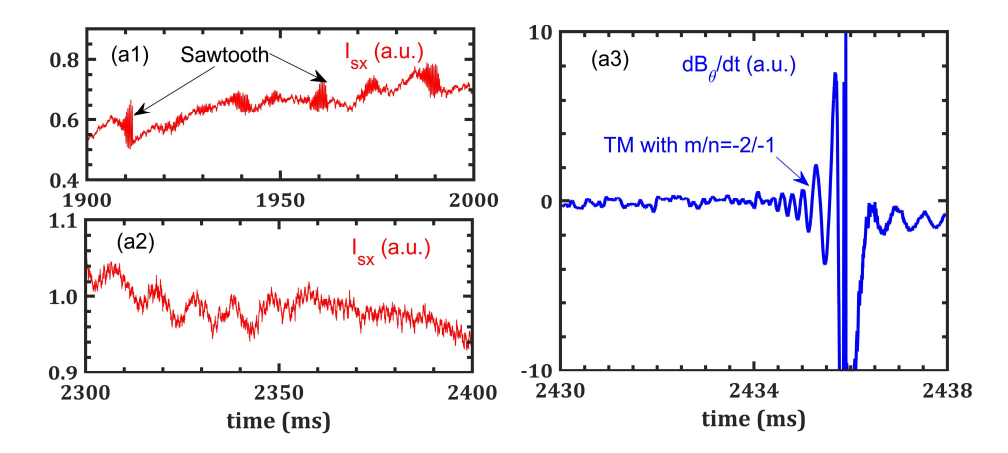


FIG. 3: (a1) Raw signal of SXR level I_{SX} for shot #38522. The black arrows indicate the moments of sawtooth crashes. (a2) Raw signal of SXR level I_{SX} for shot #38522. (a3) Raw signal of time-differential poloidal magnetic perturbation dB_{θ}/dt for shot #38522. The blue arrow indicates the moment that tearing mode (TM) with mode number m/n=-2/-1 occurs.

Identifation of KBM/AITG and their influence.—The figure 4 is the Hugill plot[14] of HL-2A high density ohmic-heated plasma. The red scatter points come from discharge with the core-localized MHD modes and blue scatter points come from discharge without the core-localized MHD modes. It is obvious that these core-localized MHD modes have a threshold of Greenwald density limit fraction, which is about $0.8ne_G$ on HL-2A ohmic heating plasma. Figure 4 also shows that these core-localized MHD modes primarily occur within the range of $0.23 < q_a < 0.28$, corresponding to $3.6 < q_a < 4.3$. As indicated in figure 3, these core-localized MHD modes frequently appear in the absence of sawtooth oscillations, suggesting that when these modes occur, the core safety factor q_0 is greater than 1. Furthermore, since the final density limit disruption is triggered by m/n=-2/-1tearing modes, the core safety factor q_0 should be less than 2. Therefore, it can be inferred that the approximate safety factor profile is as follows: in the core region, $1 < q_0 < 2$, and at the edge, $3.6 < q_a < 4.3$. Moreover, due to the absence of auxiliary heating, the safety factor increases slowly and monotonically from the core to the edge. This results in a relatively small magnetic shear s = (r/q)(dq/dr) in the plasma core. This suggests that these core-localized MHD modes may be more easily excited under conditions of weak magnetic shear and high plasma density.

In order to clarify the types of core instabilities in high-density plasmas, simulations were conducted on the parameters of one of the shots. The figure 5 gives the density ne and electron temperature Te and safety factor q profile at 1020 ms of discharge #38524. The spectrum of microwave interferometer signal for discharge #38524 is also shown in figure 5(b). Notably, in figure 5(a), the black solid line denotes the safety factor profile. As can be seen, the safety factor profile for shot #38524 exactly conforms to the case of the safety factor profile described above. At 1020 ms, there is an instability whose frequency is about 90 kHz. The parameters obtained from the profiles in figure 5 are substituted into the GENE[15] code for solution. The figure 6 is the result of growth rate γ and real frequency f versus normalized poloidal wavenumber $k_{\theta}\rho_{s}$. And the different color lines in figure 6 indicate different normalized radius ρ . KBM/AITG is found to be unstable under parameters of discharge #38524 at 1020 ms. The growth rate calculation results shown in figure 6(a) also demonstrate that KBM/AITG can exist over a broad

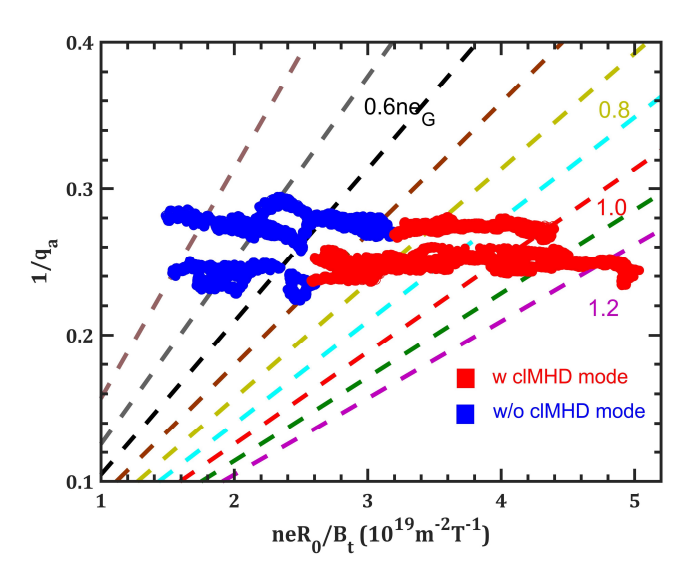


FIG. 4: Hugill plot of HL-2A high density ohmic heating plasma. q_a is the safety factor at the location r=a. The dashed lines in plot indicates relationship with Greenwald density limit and the red scatter points come from plasma with core-localized MHD modes and blue scatter points come from plasma without core-localized MHD modes.

radial range, for instance, within the region of $0.15 < \rho < 0.4$. The maximum growth rate located at $k_{\theta}\rho_{s} \sim 0.25$ at $\rho = 0.25$ and the corresponding real frequency is about 32 kHz. The difference between instabilities in figure 5(b) and figure 6(b) comes from Dopper shift effect. The simulation results of GENE code exhibit an eigenmode form, meaning that the frequency varies little across different radial positions, which is also consistent with the spectral characteristics shown in figure 5(b).

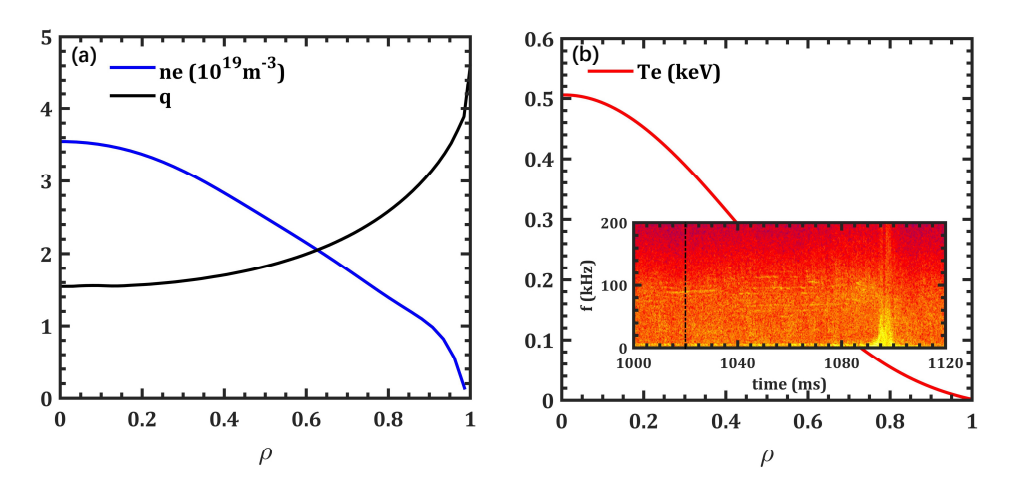


FIG. 5: a) Density ne profile and safety factor q profile for shot #38524 at 1020 ms. (b) Electron temperature Te profile provided by ECE and spectrum of microwave interferometer signal. The moment indicated by the black dashed line is the time corresponding to the profiles shown in the figure. The frequency of instability at 1020 ms is ~ 90 kHz.

Given that the experimental conditions for shot #38522 and shot #38524 closely resemble each other, and considering that the instabilities observed in these two shots display analogous characteristics and exhibit closely spaced frequencies on the microwave interferometer spectrum, it can be concluded that the instability depicted in Figure 2(b) is also attributable to KBM/AITG. Although KBM/AITG has been frequently observed

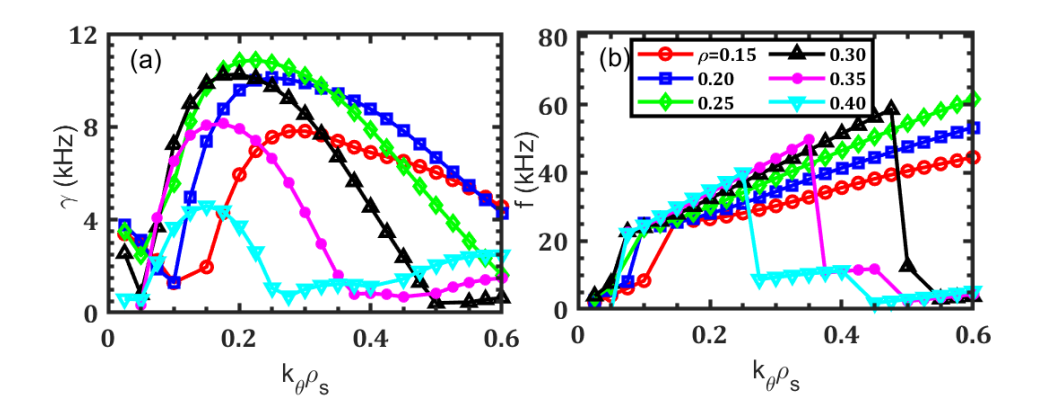


FIG. 6: (a) Growth rate γ of instability versus normalized poloidal wavenumber $k_{\theta}\rho_s$ calculated by GENE code, here ρ_s is the ion larmor radius. (b) Real frequency f of instability versus normalized poloidal wavenumber $k_{\theta}\rho_s$. The input parameters of GENE code come from profiles of discharge #38524 at 1020 ms. The different colors indicate different normalized radius $\rho = r/a$.

to occur prior to density limit disruptions in the HL-2A tokamak, its precise role in the process of density limit disruptions remains unknown.

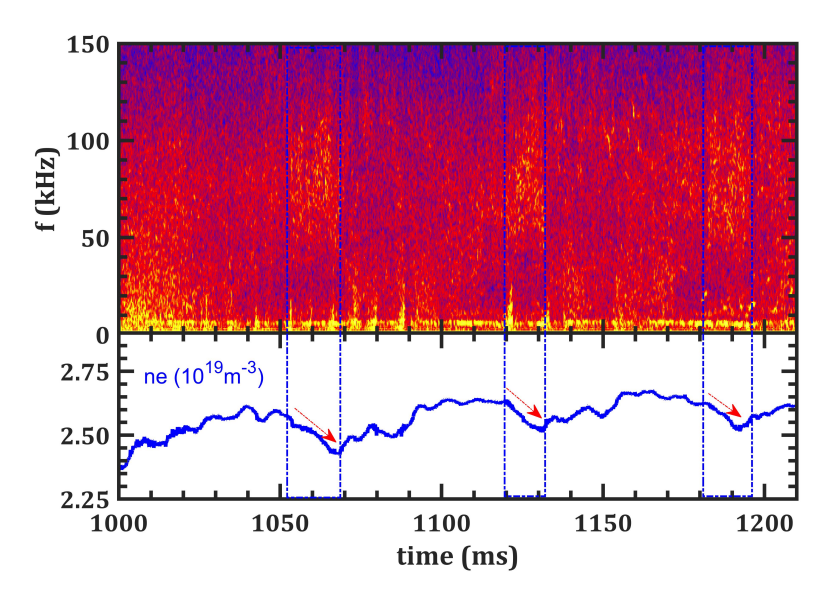


FIG. 7: Spectrum of microwave interferometer signal and corresponding density timeseries plot (blue line) for discharge #38638. The blue dashed lines indicate the time range during which core localized modes appear, while the red arrows show the trend of changes in the line-averaged plasma density following the emergence of these core localized modes.

Evidence of the influence of KBM/AITG on electron transport has also been observed on HL-2A. The figure 7 shows the spectrum of microwave interferometer signal and corresponding density time-series plot for discharge #38638. KBM/AITGs are found in the spectrum which are marked with blue dashed lines. When these KBM/AITGs appear, the line-average density of plasma decreases. The possible reason for decrease of plasma density is that KBM/AITGs lead to enhancement of particle transport in plasma core. This indicates that KBM/AITGs play a role in limiting the further increase of the plasma density. This also explains why, in figure 1, despite the continuous gas puffing

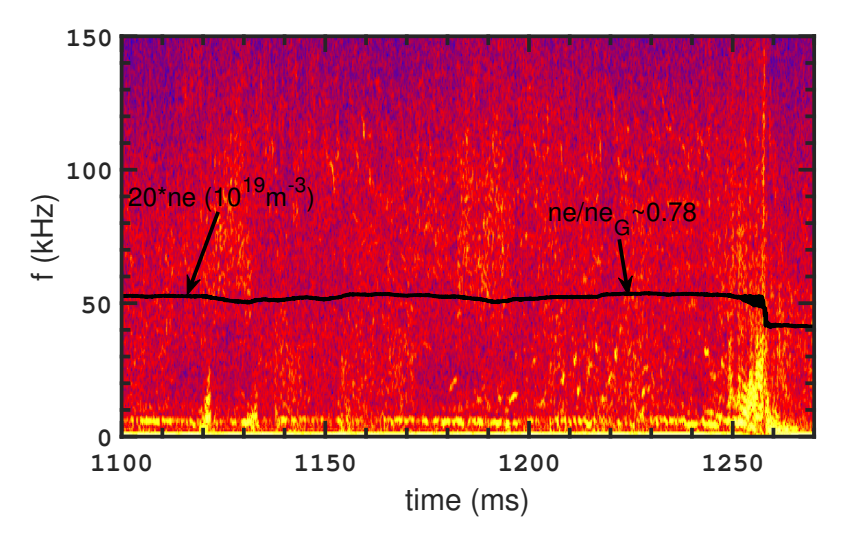


FIG. 8: Spectrum of microwave interferometer signal for shot #38638. The black lines in figure are 20 times of density 20*ne and the unit is $10^{19}m^{-3}$. The black arrows indicates the moments that 'christmas lights' modes occur.

(GP), the plasma line-averaged density ne ceases to increase further and instead maintains equilibrium after approximately 2100 ms. Coincidentally, in the microwave interferometer spectrum of figure 2(b), various instabilities including KBM/AITG begin to emerge around the same time, at approximately 2100 ms.

A density-limit-related minor disruption also occurred in shot #38638, as shown in figure 8. At approximately 1257 ms, a minor disruption takes place, characterized by a sudden drop in the plasma line-averaged density and the emergence of numerous low-frequency modes in the microwave interferometer spectrum. There are also some 'christ-mas lights' modes (KBM/AITG) occur when the density limit fraction $ne/neG \sim 0.78$, as indicated by black arrow in figure 8[16, 17]. This indicates that there is a certain connection between KBM/AITGs and density-limit-related minor disruptions.

Summary.—In the ohmic heating plasma within the HL-2A tokamak, exceeding the Greenwald density limit was achieved through gas-puffing. The maximum Greenwald density limit fraction $ne/ne_G \sim 1.3$, and the corresponding duration time is $t \sim 500$ ms $\sim 30\tau_E$. As gas injection leads to an increase in the average density, the density profile exhibits a self-organized peaking phenomenon. Instabilities emerge prior to major disruptions or minor disruptions and may serve as one of the contributing factors to these disruptions. By comparing the changes in SXR signals, magnetic probe signals, and density profiles, it was found that these instabilities are driven in the core region of plasma and they are more prone to being excited under conditions of weak magnetic shear.

The instability modes have been identified as the KBM/AITG by GENE code. Furthermore, a statistical analysis of experimental data revealed that the excitation of these modes is associated with a specific threshold fraction of the Greenwald density limit, which is $ne/ne_G \sim 0.8$ on HL-2A ohmic heating plasma. Experimentally, evidence has also been uncovered indicating that the KBM/AITGs directly lead to a reduction in the average plasma density. Consequently, the KBM/AITGs play a pivotal role in constraining the increase of plasma density in high-density ohmic heating plasmas. These new findings are of great importance to figure out and understand the origin of the density limit.

Acknowledgments.— This work is supported in part by the ITER-CN under Grants Nos. 2019YFE03020000, by NSFC under Grants No. 12125502, by SWIP innovation

under Grants No. 202301XWCX001.

References

- [1] Greenwald. M. et al. A new look at density limits in tokamaks. *Nuclear Fusion*, 28(12):2199–2207, 1988.
- [2] Greenwald. M. Density limits in toroidal plasmas. *Plasma Physics and Controlled Fusion*, 44(8):R27–R53, 2002.
- [3] White. R. B. et al. Thermal island destabilization and the Greenwald limit. *Physics of Plasmas*, 22(2):022514, 2015.
- [4] Gates. D. A. et al. Origin of tokamak density limit scalings. *Physical Review Letters*, 108(16):165004, 2012.
- [5] Chen.W. et al. Alfvénic ion temperature gradient activities in a weak magnetic shear plasma. *Europhysics Letters*, 116(4):45003, 2016.
- [6] Connor. J. W. et al. Shear, periodicity, and plasma ballooning modes. *Physical Review Letters*, 40(6):396–399, 1978.
- [7] Belli. E. A. et al. Fully electromagnetic gyrokinetic eigenmode analysis of high-beta shaped plasmas. *Physics of Plasmas*, 17(11):112314, 2010.
- [8] Kumar. N. et al. Turbulent transport driven by kinetic ballooning modes in the inner core of jet hybrid h-modes. *Nuclear Fusion*, 61(3):036005, 2021.
- [9] Nazikian. R. et al. Toroidal Alfvén eigenmodes in TFTR deuterium—tritium plasmas. *Physics of Plasmas*, 5(5):1703–1711, 1998.
- [10] Chen. W. et al. Core-localized Alfvénic modes driven by energetic ions in HL-2A NBI plasmas with weak magnetic shears. *Nuclear Fusion*, 56(3):036018, 2016.
- [11] Chen. W. et al. Kinetic electromagnetic instabilities in an ITB plasma with weak magnetic shear. *Nuclear Fusion*, 58(5):056004, 2018.
- [12] Hou. Y. W. et al. NIMROD calculations of energetic particle driven toroidal Alfvén eigenmodes. *Physics of Plasmas*, 25(1):012501, 2018.
- [13] Wesson. J. et al. Tokamaks, volume 149. Oxford university press, 2011.
- [14] Stabler. A. et al. Density limit investigations on ASDEX. *Nuclear Fusion*, 32(9):1557–1583, 1992.
- [15] Jenko. F. et al. Electron temperature gradient driven turbulence. *Physics of Plasmas*, 7(5):1904–1910, 2000.
- [16] Heidbrink. W.W. et al. 'BAAE' instabilities observed without fast ion drive. *Nuclear Fusion*, 61(1):016029, 2021.
- [17] Ma. R. R. et al. Low-frequency shear Alfvén waves at DIII-D: Theoretical interpretation of experimental observations. *Physics of Plasmas*, 30(4), 2023.